Physiological Reports

Open Access

Physiological Reports ISSN 2051-817X

ORIGINAL RESEARCH

Functional respiratory imaging, regional strain, and expiratory time constants at three levels of positive end expiratory pressure in an ex vivo pig model

William R. Henderson[1], Yannick Molgat-Seon[2], Wim Vos[3], Rachel Lipson[4], Francisca Ferreira[3], Miranda Kirby[5], Cedric Van Holsbeke[3], Paolo B. Dominelli[6], Donald E. G. Griesdale[6], Mypinder Sekhon[7], Harvey O. Coxson[8], John Mayo[9] & A. William Sheel[6]

1 Division of Critical Care Medicine, Vancouver General Hospital, Vancouver, British Columbia, Canada
2 School of Kinesiology, Vancouver, Canada
3 FluidDA, Leuven, Belgium
4 Emmes Canada, Vancouver, Canada
5 Radiology, The University of British Columbia, Vancouver, British Columbia, Canada
6 School of Kinesiology, University of British Columbia, Vancouver, British Columbia, Canada
7 Division of Critical Care Medicine, Vancouver General Hospital, Vancouver, British Columbia, Canada
8 Centre for Heart Lung Innovation, St Paul's Hospital, University of British Columbia, Vancouver, British Columbia, Canada
9 Department of Radiology, Vancouver General Hospital, University of British Columbia, Vancouver, British Columbia, Canada

Keywords
Positive end-expiratory pressure, strain, time constant.

Correspondence
William Henderson, Division of Critical Care Medicine, Vancouver General Hospital, ICU2, JPPN 2nd Floor, Room 2438, 855 West 12th Avenue, Vancouver, BC, Canada V5Z 1M9
Tel: 604-875-5949
Fax: 604-875-5957
E-mail: william.henderson@vch.ca

Funding Information
WRH was supported by a four year fellowship from the University of British Columbia. WRH and DEEG were supported by Clinician Scientist Awards from the VGH and UBC Best of Health Fund. YMS and PBD were supported by four-year fellowships from the University of British Columbia and doctoral scholarships from the Natural Science and Engineering Research Council. HOC is supported by the BC Lung Association Robert R Miller Fellowship in Thoracic Imaging. MK gratefully acknowledges support from the Canadian Institutes of Health Research Banting Fellowship Program.

Received: 7 October 2016; Revised: 28 October 2016; Accepted: 5 November 2016

doi: 10.14814/phy2.13059

Physiol Rep, 4 (23), 2016, e13059, doi: 10.14814/phy2.13059

Abstract

Heterogeneity in regional end expiratory lung volume (EELV) may lead to variations in regional strain (ε). High ε levels have been associated with ventilator-associated lung injury (VALI). While both whole lung and regional EELV may be affected by changes in positive end-expiratory pressure (PEEP), regional variations are not revealed by conventional respiratory system measurements. Differential rates of deflation of adjacent lung units due to regional variation in expiratory time constants (τ_E) may create localized regions of ε that are significantly greater than implied by whole lung measures. We used functional respiratory imaging (FRI) in an ex vivo porcine lung model to: (i) demonstrate that computed tomography (CT)-based imaging studies can be used to assess global and regional values of ε and τ_E and, (ii) demonstrate that the manipulation of PEEP will cause measurable changes in total and regional ε and τ_E values. Our study provides three insights into lung mechanics. First, image-based measurements reveal egional variation that cannot be detected by traditional methods such as spirometry. Second, the manipulation of PEEP causes global and regional changes in R, E, ε and τ_E values. Finally, regional ε and τ_E were correlated in several lobes, suggesting the possibility that regional τ_E could be used as a surrogate marker for regional ε.

Introduction

Mechanical ventilation is used in the care of surgical and medically ill patients. Current best practice assesses management of mechanical ventilation based on indices of oxygenation or on aggregate measures of pulmonary function such as pressure–volume curves or transpulmonary pressure (ARDSNetwork 2000; Brower et al. 2004; Guérin 2013; Goligher et al. 2014). While pragmatic, these strategies do not account for regional variation in lung tissue parameters such as strain (ε), a crucial determinant of local lung injury (Eissa et al. 1991; Schiller et al. 2001; Hickling 2002; Otto et al. 2008; Mertens et al. 2009; Loring et al. 2010; Kaczka et al. 2011*a*,*b*). Strain (ε) is the ratio of tidal volume (V_T) to end-expiratory lung volume (EELV). High ε levels have been associated with ventilator-associated lung injury (VALI) (Protti et al. 2011; González-López et al. 2012). The heterogeneity in regional EELV due to atelectasis may lead to variations in regional ε (Cressoni et al. 2014). While both whole lung and regional EELV may be affected by changes in positive end-expiratory pressure (PEEP), regional variations are not revealed by conventional respiratory system measurements.

The ratio of the resistance (R) to elastance (E) of a lung unit during passive deflation is, defined as the expiratory time constant (τ_E). Differential rates of deflation of adjacent lung units due to regional variation in τ_E may create localized regions of ε that are significantly greater than implied by whole lung measures of pressure or ε (Mead et al. 1970; Kaczka et al. 2011*a*; Perchiazzi et al. 2011; Cressoni et al. 2014).

In recent studies, functional respiratory imaging (FRI) information has been obtained by combining anatomic computed tomography (CT) images with functional information calculated using computational fluid dynamics (CFD). To achieve this, numerical flow equations (Navier-Stokes equations) are solved in subject-specific computational grids, based on segmented three-dimensional models of the airways and lungs, using subject-specific boundary conditions (Lin et al. 2009; De Backer et al. 2008). The result of FRI is a local description of volume, pressure and flow characteristics throughout the entire respiratory system, which has proven to be more sensitive than conventional lung function measures (De Backer et al. 2012; Vos et al. 2013). Furthermore, FRI provides novel insights in the mode of action of new compounds that have effects that are hard to analyze via traditional lung function testing (De Backer et al. 2014; Vos et al. 2016). Thus, FRI provides a method by which local ε and τ_E values may be assessed.

Our understanding of the complexities of how PEEP causes regional changes in strain and tau is incomplete and advances have been methodologically limited. As such, the purpose of this study was to use a novel imaging method to assess regional values of ε and τ_E and test the hypothesis that changes in PEEP would have distinct effects on a per lobe basis. To this end, we used FRI in an ex-vivo porcine lung model to: (i) demonstrate that CT-based imaging studies can be used to assess global and regional values of ε and τ_E and, (ii) demonstrate that the manipulation of PEEP will cause measurable changes in total and regional ε and τ_E values.

Methods

Ethical approval

All experiments were approved by the Animal Research Committee of the University of British Columbia, Vancouver, British Columbia and conformed guidelines outlined by the Physiological Society (Grundy 2015).

Ex-vivo lung preparation

After participation in a surgical skills training session, euthanasia with pentobarbital sodium (120 mg kg^{-1} intravenous) was achieved in five adult female Yorkshire X pigs. Death was confirmed by the absence of a pulse and cardiac electrical activity on continuous surface electrocardiography. The lungs and trachea of were removed *en block* through a sternal incision, and an endotracheal tube (9.0 mm internal diameter) was placed into the trachea. The lungs and trachea were then suspended from a nonmetallic scaffold inside of a CT scanner (Aquilion One Volumetric CT scanner; Toshiba Medical Systems, Tustin, CA). The lungs were then initially ventilated (Puritan-Bennett 7200; Covidien, Dublin, Ireland) with 0 cm H_2O of PEEP, using a fraction of inspired oxygen of 0.21, V_T of 6 mL kg^{-1} of body weight, and a breathing frequency (f_b) of 12 breaths min^{-1}. Inspiratory and expiratory flows ($\dot{V}_I$ and $\dot{V}_E$) were measured using a heated pneumotachograph (Model 3813; Hans Rudolph, Shawnee, KS) placed between the ventilator tubing wye and the proximal end of the endotracheal tube. Inspiratory flows were held constant at 45 L min^{-1} with a square waveform. The pneumontachometer was calibrated with a 1 L calibration syringe prior to each trial. Inspiratory and expiratory volumes (V_I and V_E) were obtained by numerical integration of the flow signals.

Intervention

The lungs were ventilated as described above with PEEP levels of 0, 5 and 10 cm H_2O. The order of PEEP levels

was randomly assigned, and 10 min of ventilation at each PEEP level occurred prior to recording images and physiological data.

Image acquisition and processing

All lungs underwent CT imaging at multiple time points during inflation and deflation on the mechanical ventilator. Imaging was performed with the lung suspended in the upright position and was gated to begin at the beginning of inflation and end at the cessation of inflation. The CT settings were as follows: tube voltage, 120 kV; tube current, 200 mAs; rotation time, 0.35 sec; field of view, 400.4 mm; slice thickness, 0.50 mm; pixel spacing 0.782 mm; and convolution kernel, FC51. The images were acquired without moving the table (pitch: 0) and the acquisition began immediately prior to lung inflation and concluded after complete cessation of gas flow following passive deflation. Imaging data was converted into 3D models of airways and lung lobes using Mimics 15 (Materialise, Leuven, Belgium) a previously validated software package (Food and Drug Administration, K073468; Conformité Européenne certificate, BE 05/1191.CE.01) (Video 1). Airways were segmented using directional thresholding with automated leakage detection. Lungs were split into lobes by identification of the fissure lines from the CT scan. For both airway and lung lobe segmentation, manual updating of the automated algorithms was performed when needed. Lungs lobes and the respiratory tract could be extracted at several time points during inflation and deflation (Fig. 1). For data analysis, we used the end-expiratory scan for both lobar and airway analysis and the end-inspiratory scan for lobar analysis only.

We identified lobes as follows: right and left anterior lobes (RAL and LAL), right and left caudal lobes (RCL and LCL), right and left diaphragmatic lobes (LDL and LDL), and the right internal lobe (RIL) (Fig. 1). Airways were trimmed perpendicular to the local centerline in order to prepare the model for CFD airflow analysis. Airway models were split into a central part and airways leading to each previously defined lobe (Fig. 1).

Calculation of strain and time constant values using CT data

Using the derived 3D lobar models, we calculated the volume of each lobe at end-inspiratory lung volume (EILV) and EELV. Regional ε for each lobe was calculated as follows: (EILV − EELV)/EELV using the appropriate lobar volumes. For example, the ε of the RDL (ε_{RDL}) was calculated as $(EILV_{RDL} - EELV_{RDL})/EELV_{RDL}$. Total respiratory system EELV ($EELV_{RS}$) and EILV ($EILV_{RS}$) were calculated by determining the sum of all lobar volumes. Total respiratory system ε (ε_{RS}) was calculated as follows: $(EILV_{RS} - EELV_{RS})/EELV_{RS}$.

Expiratory time constants were calculated by determining the quotient of R and E. Resistance was defined as the total pressure drop needed to drive flow through an airway section. Regional airflow was obtained from the total airflow ($(EILV_{RS} - EELV_{RS})$/time of deflation) combined with the internal airflow distribution calculated on a lobar basis by: $(EILV_{RDL} - EELV_{RDL})/(EILV_{RS} - EELV_{RS})$. Expiratory laminar steady CFD calculations were carried out using velocity inlets (inlet velocity = flow rate through region/total area of inlet in the region) at the terminal bronchi and a pressure outlet (total pressure = PEEP) at the trachea. From the CFD calculation, the pressure drop over each specific lobar region was obtained. Elastance was defined as the pressure change needed to obtain a known volume. The volume change was given by EILV-EELV and the pressure change was the pressure drop in the trachea throughout deflation. CFD simulations were performed in Fluent 14.0 (Ansys Inc, Canonsburg, PA).

Statistical analysis

For lobe-specific models, lobe, PEEP and their interaction were included as main effects with a random effect for pig included to account for the possibility of intra-animal correlation. Testing for significance of fixed effects was done with *F*-Tests and type III sums of squares. Total lung measurements were not included in lobe-specific models and were modeled separately, using a similar approach. All testing of differences in least squared means was adjusted for multiple comparisons, using the Tukey–Kramer method. *P*-values less than 0.05 were considered significant.

Separate mixed effect models to assess the relationship between tau and strain were fit for each lobe and for the total lung so that separate R^2 values could be obtained. Each model included τ_E as the response, ε as the predictor, and a random effect for pig. The pseudo-R^2 value $R^2_{LMM(m)}$, proposed by Nakagawa and Schielzeth for mixed effects models (Nakagawa and Schielzeth 2013), is reported for each lobe and for the entire lung in Figure Y, where $R^2_{LMM(m)}$ measures the proportion of the variance of τ_E explained by ε based on the fitted mixed effect model. $R^2_{LMM(m)}$ values of 1 indicate perfect correlation between tau and strain, while a value of 0 indicates no correlation between them. Testing the significance of the relationship between tau and strain was performed with *F*-tests and type III sums of squares, and the Benjamini–Hochberg significance level was used to determine if the relationship between τ_E and ε was statistically significant while adjusting for multiple comparisons.

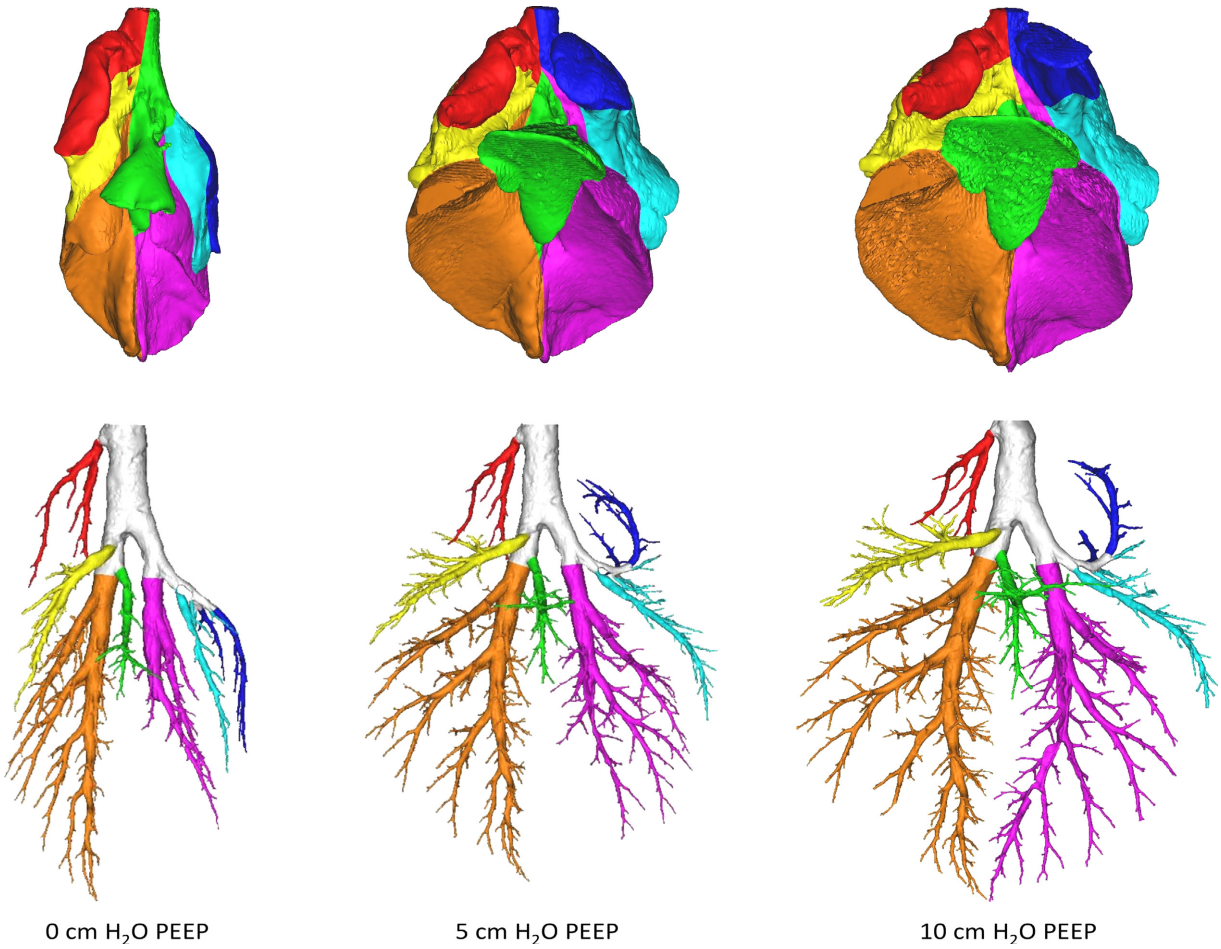

Figure 1. Pictoral representation of lung lobes and airways using composite 3D airway images at three positive end expiratory pressures. PEEP 0/5/10, positive end expiratory pressure of 0/5/10 cm H_2O. Red, right anterior lobe; Yellow, right caudal lobe; Orange, right diaphragmatic lobe; Green, right internal lobe; Purple, left diaphragmatic lobe; Light blue, left caudal lobe; Dark blue, left anterior lobe.

Results

Global resistance, elastance, strain and time constants

When considering the whole respiratory system using FRI, R, E, ε and τ_E were all affected by PEEP ($P < 0.05$ for each). After adjusting for multiple comparisons, R at PEEP 0 was significantly higher than at PEEP 10 ($P < 0.05$). Elastance was significantly higher at PEEP 10 compared to PEEP 0 and 5 ($P < 0.01$), ε was higher at PEEP 0 than at PEEP 5 or 10 ($P < 0.05$), and τ_E at PEEP 0 and 5 was significantly higher than at PEEP 10 ($P < 0.05$).

Regional resistance, elastance, strain and time constants

In the model including lobe, R was affected by PEEP, lobe, and the interaction of PEEP and lobe ($P < 0.0001$); higher PEEP resulted in reduced resistance, but the effect of PEEP on R differed between lobes. Data regarding R values per PEEP setting and per lobe are in Figures 2 and 3, respectively. Specifically, R in LAL was significantly different from all other lobes ($P < 0.0001$) and R at PEEP 0 was significantly higher than PEEP 5 and 10 ($P < 0.01$).

Elastance was different for different levels of PEEP (Fig. 4, $P < 0.01$) and lobe (Fig. 5, $P < 0.0001$), but the interaction was not significant ($P = 0.18$); the relationship between PEEP and lobe was similar for all lobes. However, some specific differences did exist: E in RAL was significantly higher than in LAL, LCL, LDL, RCL, and RDL ($P < 0.01$) and was greater in RIL than in LDL and RDL ($P < 0.01$). In addition, E was significantly higher at PEEP 10 than at PEEP 0 or 5 ($P < 0.05$).

Strain was affected by PEEP (Fig. 6, $P < 0.05$) and lobe (Fig. 7, $P < 0.0001$) but not by the interaction of PEEP and lobe ($P = 0.57$). RAL was found to be significantly different from LAL and RDL with respect to ε ($P < 0.05$).

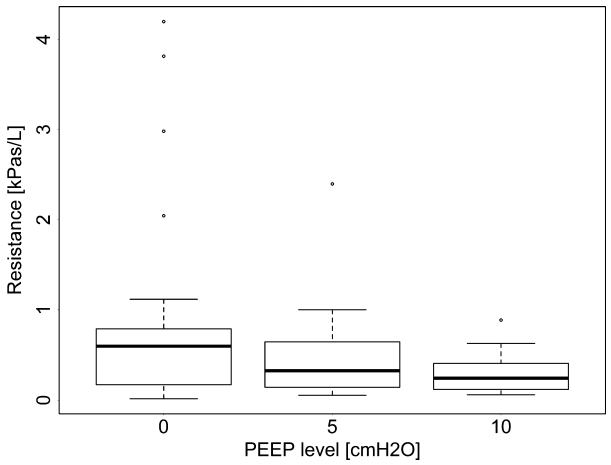

Figure 2. The effect of positive end expiratory pressure (PEEP) in expiratory resistance as calculated by functional respiratory imaging (FRI). The extremes of the box represent the quartiles and the black line represents the median. The whiskers extend to the most extreme data point which is no more than 1.5 times the interquartile range from the box. Open circles represent data points outside of this range.

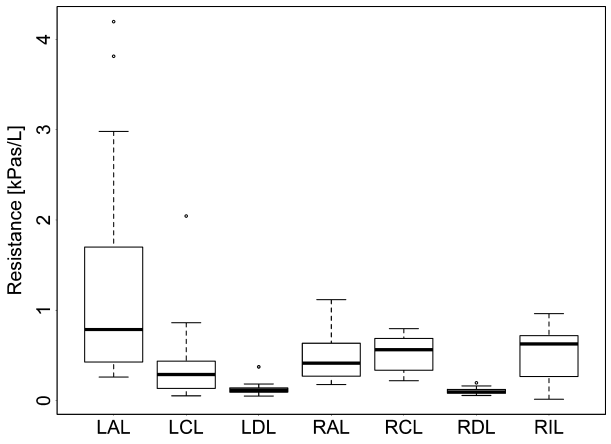

Figure 3. The effect of lobe on expiratory resistance as calculated by functional respiratory imaging (FRI). RAL, right anterior lobe; RCL, right caudal lobe; RDL, right diaphragmatic lobe; RIL, right internal lobe; LDL, left diaphragmatic lobe; LCL, left caudal lobe; LAL, left anterior lobe. The extremes of the box represent the quartiles and the black line represents the median. The whiskers extend to the most extreme data point which is no more than 1.5 times the interquartile range from the box. Open circles represent data points outside of this range.

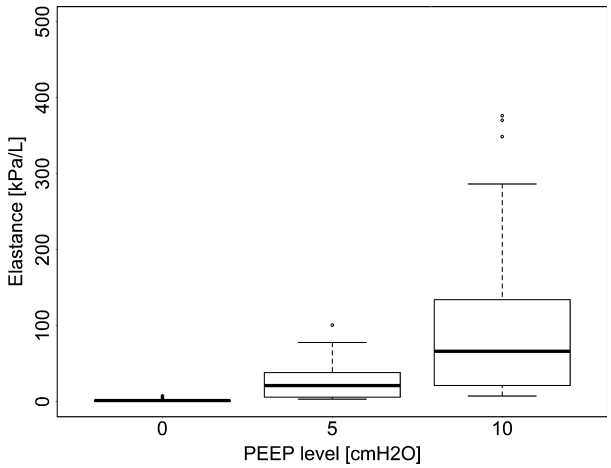

Figure 4. The effect of positive end expiratory pressure (PEEP) in lung elastance as calculated by functional respiratory imaging (FRI). The extremes of the box represent the quartiles and the black line represents the median. The whiskers extend to the most extreme data point which is no more than 1.5 times the interquartile range from the box. Open circles represent data points outside of this range.

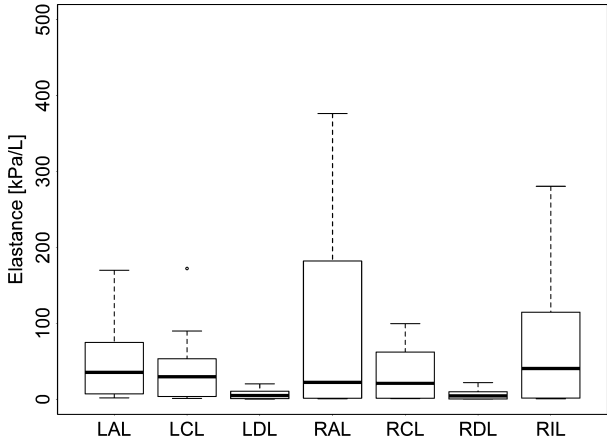

Figure 5. The effect of lobe in lung elastance as calculated by functional respiratory imaging (FRI). RAL, right anterior lobe; RCL, right caudal lobe; RDL, right diaphragmatic lobe; RIL, right internal lobe; LDL, left diaphragmatic lobe; LCL, left caudal lobe; LAL, left anterior lobe. The extremes of the box represent the quartiles and the black line represents the median. The whiskers extend to the most extreme data point which is no more than 1.5 times the interquartile range from the box. Open circles represent data points outside of this range.

Strain was highest at PEEP 0 compared to 5 and 10 ($P < 0.0001$) and was also higher at PEEP 5 than at PEEP 10 ($P < 0.05$).

Consistent with the relationship of τ_E to R, τ_E values were affected by PEEP (Fig. 8, $P < 0.01$), lobe (Fig. 9, $P < 0.01$) and the interaction between PEEP and lobe ($P < 0.05$). The values of τ_E in LAL was also significantly higher than in all other lobes ($P < 0.05$) and τ_E was higher at PEEP 0 than at PEEP 5 or 10 ($P < 0.05$).

Relationship between strain and time constants

After adjusting for multiple comparisons, there was evidence of a relationship between τ_E and ε in lobes LAL,

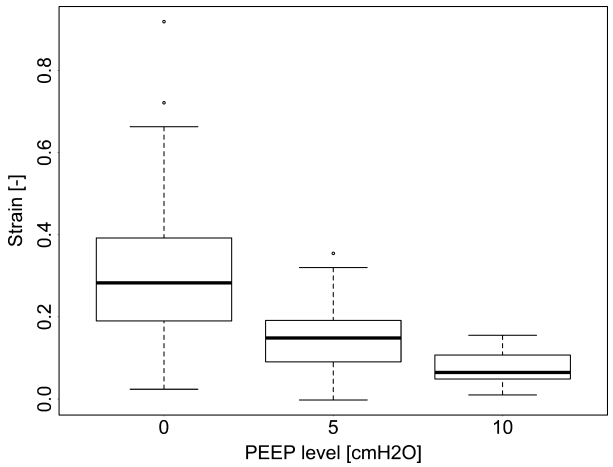

Figure 6. The effect of positive end expiratory pressure (PEEP) on strain as calculated by functional respiratory imaging (FRI). The extremes of the box represent the quartiles and the black line represents the median. The whiskers extend to the most extreme data point which is no more than 1.5 times the interquartile range from the box. Open circles represent data points outside of this range.

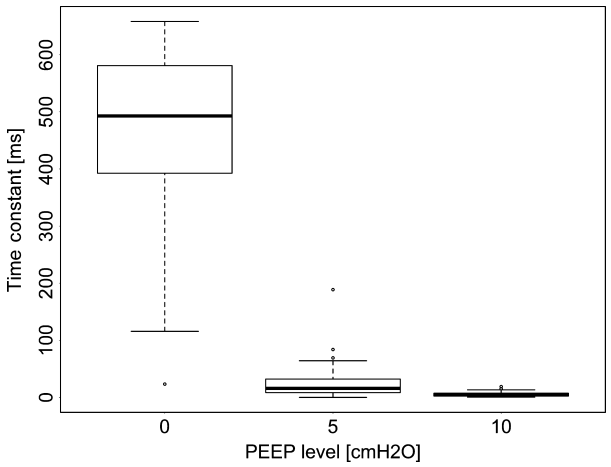

Figure 8. The effect of positive end expiratory pressure (PEEP) on the expiratory time constant as calculated by functional respiratory imaging (FRI). The extremes of the box represent the quartiles and the black line represents the median. The whiskers extend to the most extreme data point which is no more than 1.5 times the interquartile range from the box. Open circles represent data points outside of this range.

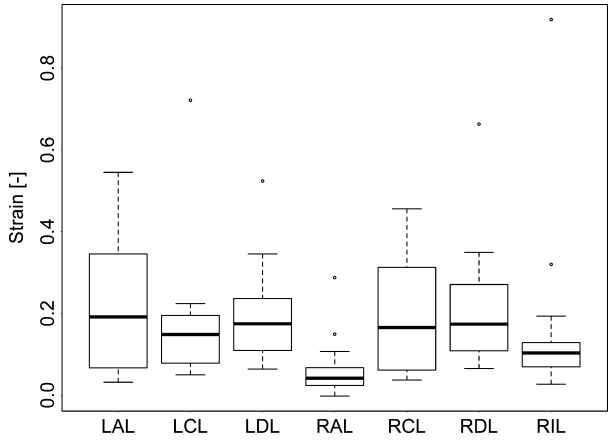

Figure 7. The effect of lobe on strain as calculated by functional respiratory imaging (FRI). RAL, right anterior lobe; RCL, right caudal lobe; RDL, right diaphragmatic lobe; RIL, right internal lobe; LDL, left diaphragmatic lobe; LCL, left caudal lobe; LAL, left anterior lobe. The extremes of the box represent the quartiles and the black line represents the median. The whiskers extend to the most extreme data point which is no more than 1.5 times the interquartile range from the box. Open circles represent data points outside of this range.

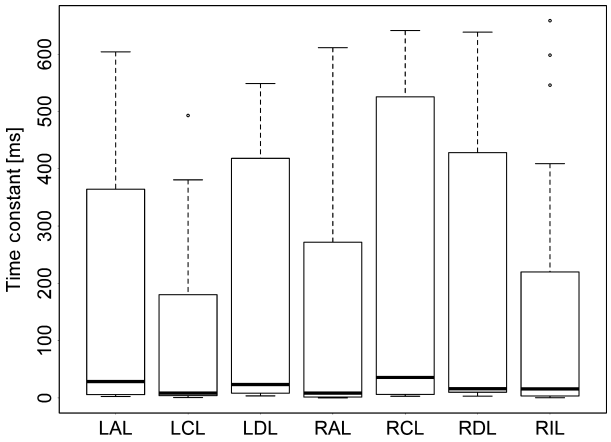

Figure 9. The effect of lobe on the expiratory time constant as calculated by functional respiratory imaging (FRI). RAL, right anterior lobe; RCL, right caudal lobe; RDL, right diaphragmatic lobe; RIL, right internal lobe; LDL, left diaphragmatic lobe; LCL, left caudal lobe; LAL, left anterior lobe. The extremes of the box represent the quartiles and the black line represents the median. The whiskers extend to the most extreme data point which is no more than 1.5 times the interquartile range from the box. Open circles represent data points outside of this range.

LCL, RAL, RCL, and RIL ($P < 0.01$, Benjamini–Hochberg significance level 0.03). The pseudo-R^2 between τ_E and ε was high in lobes LCL and RAL ($R^2_{LMM(m)} > 0.9$), moderate in lobes LAL, RCL, and RIL ($0.4 < R^2_{LMM(m)} > 0.9$) and low in lobes LDL, RDL, and in the total lung measurement ($R^2_{LMM(m)} < 0.2$).

Discussion

Our study used FRI to quantify differences between global and regional values of R, E, ε and τ_E and provides three insights into lung mechanics. First, image-based

measurements reveal regional variation that cannot be detected by traditional methods such as spirometry. Second, the manipulation of PEEP causes global and regional changes in R, E, ε and τ_E values. Finally, regional ε and τ_E were correlated in several lobes, suggesting the possibility that regional τ_E could be used as a surrogate marker for regional ε. In sum, our experimental findings provide insight into the physiological complexities of mechanical ventilation where we found that PEEP causes significant regional differences in resistance, strain and expiratory time constants that are not detectable with conventional methods.

Global and regional strain with FRI

Recognition of the deleterious effects of large V_T during mechanical ventilation has increased over the last twenty years, with recommendations to minimize V_T in an attempt to minimize ε_{RS} (ARDSNetwork 2000). Recent studies (Chiumello et al. 2008; Protti et al. 2011) have shown that ε_{RS} is a primary driver of VALI, and that V_T is a poor surrogate for ε_{RS} (Gattinoni et al. 2003; Santana et al. 2009; González-López et al. 2012). Therefore, to mitigate VALI, investigators have attempted to more accurately measure important mechanical parameters of the lung such as ε. Our results demonstrate that ε_{RS} decreased with increasing PEEP, an observation that has been previously documented and which was due to increased $EELV_{RS}$ in our experiment (Blankman et al. 2016). More important than the fact that the techniques described in our study allow the measurement of ε_{RS}, is the ability to observe regional ε. Heterogeneity in regional ε has previously been observed using methods such as CT scans, electrical impedance plethysmography and forced oscillation techniques (Kaczka et al. 2011*b*; Pulletz et al. 2012; Wolf et al. 2013; Cressoni et al. 2014; da Paula et al. 2016). We found that varied widely, with the highest strain lobes exposed to approximately threefold the strain of the lowest strain lobes (Fig. 7). Both PEEP and lobe independently affected the ε measured in individual lobes. The clinical implications of interlobe variability in ε may be significant. For example, clinicians may use whole respiratory system measurements (such as ε_{RS}) in an attempt to minimize new lung injury during mechanical ventilation, but may unwittingly still subject some lung regions to high ε levels.

Global and regional time constants with FRI

During passive deflation, τ_E conveys information about pulmonary mechanics that may guide therapy (Lourens et al. 2000; Al-Rawas et al. 2013). We calculated expiratory values τ_E using this novel application of FRI. Deflation was more rapid with increases in PEEP (Fig. 8) and these decreases in τ_{ERS} were due to decreases in R, rather than increases in E (Figs. 2 and 4). Historically, methods of measuring τ_E were limited to whole lung measures based upon the assumption that the lung is isotropic, and are therefore unable to address regional differences in lung mechanics. Kaczka et al. (2005) have demonstrated that regional values of R and E (and by implication, regional values of τ_E) may vary with both f_b and pressure. Similarly, our data demonstrate that there is substantial variation in τ_E between lobes, and that this variation is not well represented by the global measure (τ_{ERS}). The significant interaction terms seen in our statistical model indicate that both PEEP and lobe affected τ_E in the per lobe analysis. The clinical implication of these findings is that some lobes may require significantly longer to fill or empty than τ_{ERS} would suggest, potentially leading to areas of shunt or deadspace. This raises that possibility that a clearer understanding of the regional variation in τ_E could guide clinicians in modifying the parameters of mechanical ventilation used in patients with significant regional variation in τ_E.

Correlation between strain and time constants

Across all PEEP levels, the correlation between τ_E and ε was very strong in lobes RAL and LCL, short τ_E correlating with small ε. This relationship was weak for the total lung and reflects that the heterogeneous nature of the relationship between τ_E and ε in the different lobes. This limited finding provides some support for the idea that regional τ_E variation could be a useful surrogate for regional ε variation. However, this possibility requires significant clarification in future studies before it has clinical utility.

Limitations

This study demonstrates the utility of FRI to measure regional heterogeneity in both ε and τ_E, but some potential limitations should be acknowledged. First, the best manner in which to calculate ε in studies of mechanical ventilation that utilize PEEP is controversial. During normal breathing without PEEP, ε is the ratio of V_T to functional residual capacity (FRC). The application of PEEP will increase the resting lung volume by some additional volume (V_{PEEP}). Several investigators have added V_{PEEP} to the distending volume and therefore calculate ε as (V_T+V_{PEEP})/FRC (Protti et al. 2009; Gattinoni et al. 2012). Underlying this method is the rationale that V_{PEEP} distends the lung beyond FRC and thereby causing deformation. Others have calculated ε as V_T/EELV, where EELV includes both FRC and V_{PEEP} (Mentzelopoulos

et al. 2005; Brunner and Wysocki 2009; da Paula et al. 2016). The latter approach was used in this study for two reasons. First, stress relaxation may allow the lungs to achieve a new resting volume (that is without ε at end-expiration at different PEEP levels) (Fuld et al. 2008). Recent analyses that indicate that static deformation due to ε (due to PEEP) may be less injurious than dynamic volume changes due to ε (from V_T) support this view (Protti et al. 2013). Moreover, the principal utility of strain calculations is to mitigate new lung injury, particularly in patients with significant lung injury or acute respiratory distress syndrome. It is difficult to measure EELV in these PEEP-dependent patients due to the risk of hypoxemia when PEEP is removed. This study thus replicates the clinical reality in the treatment of such patients. Finally, this study occurred in cadaveric lungs that were not contained within a chest wall. In this situation both EELV and E_{RS} will be lower than in intact subjects. These factors will increase ε measurements (particularly in the zero PEEP condition), lengthen τ_E values, and alter the distribution of lobar strains as compared to live animals. Second, in the current experimental set up, the lungs were suspended vertically as opposed to horizontally. This may have altered the interlobar ε distribution as compared to intact subjects. Finally, at end-expiration with zero PEEP, alveolar ducts and small conducting airways may be subjected to cyclic derecruitment and recruitment. This could expose them to nonlinear dynamics that would not be captured in our computational model.

Conclusion

Mechanical ventilation may precipitate VALI through the creation of high global ε. Both theory and experimental data suggest that whole lung measures of strain do not accurately represent regional pulmonary mechanics. Our data show that FRI can demonstrate the significant differences between regional and global measures of ε and τ_E. We found limited evidence that ε and τ_E are correlated. While the clinical importance of these data may be significant, further studies are required to clarify their use in clinical practice.

Conflict of Interest

All authors affirm that they have no competing interests with respect to the subject matter of this manuscript. WV is shareholder of FLUIDDA NV. CVH and FF are employed by FLUIDDA NV.

References

Al-Rawas, N., M. J. Banner, N. R. Euliano, C. G. Tams, J. Brown, A. D. Martin, et al. 2013. Expiratory time constant for determinations of plateau pressure, respiratory system compliance, and total resistance. Crit. Care 17:R23.

ARDSNetwork. 2000. Ventilation with lower tidal volumes as compared with traditional tidal volumes for acute lung injury and the acute respiratory distress syndrome. N. Engl. J. Med. 342:1301–1308.

Blankman, P., D. Hasan, I. G. Bikker, and D. Gommers. 2016. Lung stress and strain calculations in mechanically ventilated patients in the intensive care unit. Acta Anaesthesiol. Scand. 60:69–78.

Brower, R. G., P. N. Lanken, N. MacIntyre, M. A. Matthay, A. Morris, M. Ancukiewicz, et al. 2004. Higher versus lower positive end-expiratory pressures in patients with the acute respiratory distress syndrome. N. Engl. J. Med. 351:327–336.

Brunner, J. X., and M. Wysocki. 2009. Is there an optimal breath pattern to minimize stress and strain during mechanical ventilation? Intensive Care Med. 35:1479–1483.

Chiumello, D., E. Carlesso, and P. Cadringher. 2008. Lung stress and strain during mechanical ventilation of the acute respiratory distress syndrome. J. Respir. 178:346–355.

Cressoni, M., P. Cadringher, C. Chiurazzi, M. Amini, E. Gallazzi, A. Marino, et al. 2014. Lung inhomogeneity in patients with acute respiratory distress syndrome. Am. J. Respir. Crit. Care Med. 189:149–158.

De Backer, J. W., W. G. Vos, C. D. Gorlé, P. Germonpré, B. Partoens, F. L. Wuyts, et al. 2008. Flow analyses in the lower airways: patient-specific model and boundary conditions. Med. Eng. Phys. 30:872–879.

De Backer, L. A., W. Vos, J. De Backer, C. Van Holsbeke, S. Vinchurkar, and W. De Backer. 2012. The acute effect of budesonide/formoterol in COPD: a multi-slice computed tomography and lung function study. Eur. Respir. J. 40:298–305.

De Backer, W., W. Vos, C. Van Holsbeke, S. Vinchurkar, R. Claes, A. Hufkens, et al. 2014. The effect of roflumilast in addition to LABA/LAMA/ICS treatment in COPD patients. Eur. Respir. J. 44:527–529.

Eissa, N. T., V. M. Ranieri, C. Corbeil, M. Chassé, F. M. Robatto, J. Braidy, et al. 1991. Analysis of behavior of the respiratory system in ARDS patients: effects of flow, volume, and time. J. Appl. Physiol. 70:2719–2729.

Fuld, M. K., R. B. Easley, O. I. Saba, D. Chon, J. M. Reinhardt, E. A. Hoffman, et al. 2008. CT-measured regional specific volume change reflects regional ventilation in supine sheep. J. Appl. Physiol. 104:1177–1184.

Gattinoni, L., E. Carlesso, P. Cadringher, F. Valenza, F. Vagginelli, and D. Chiumello. 2003. Physical and biological triggers of ventilator-induced lung injury and its prevention. Eur. Respir. J. 22:15s–25s.

Gattinoni, L., E. Carlesso, and P. Caironi. 2012. Stress and strain within the lung. Curr. Opin. Crit. Care 18:42–47.

Goligher, E. C., B. P. Kavanagh, G. D. Rubenfeld, N. K. J. Adhikari, R. Pinto, E. Fan, et al. 2014. Oxygenation response to positive end-expiratory pressure predicts

mortality in acute respiratory distress syndrome. A secondary analysis of the LOVS and ExPress trials. Am. J. Respir. Crit. Care Med. 190:70–76.

González-López, A., E. García-Prieto, E. Batalla-Solís, L. Amado-Rodríguez, N. Avello, L. Blanch, et al. 2012. Lung strain and biological response in mechanically ventilated patients. Intensive Care Med. 38:240–247.

Grundy, D. 2015. Principles and standards for reporting animal experiments in The Journal of Physiology and Experimental Physiology. Exp. Physiol. 100:755–758.

Guérin, C., et al. 2013. Prone positioning in severe acute respiratory distress syndrome. N. Engl. J. Med. 368:2159–2168.

Hickling, K. G. 2002. Reinterpreting the pressure-volume curve in patients with acute respiratory distress syndrome. Curr. Opin. Crit. Care 8:32–38.

Kaczka, D. W., D. N. Hager, M. L. Hawley, and B. A. Simon. 2005. Quantifying mechanical heterogeneity in canine acute lung injury. Anesthesiology 103:306–312.

Kaczka, D. W., K. Cao, G. E. Christensen, J. H. T. Bates, and B. A. Simon. 2011a. Analysis of regional mechanics in canine lung injury using forced oscillations and 3D image registration. Ann. Biomed. Eng. 39:1112–1124.

Kaczka, D. W., K. R. Lutchen, and Z. Hantos. 2011b. Emergent behavior of regional heterogeneity in the lung and its effects on respiratory impedance. J. Appl. Physiol. 110:1473–1481.

Lin, C.-L., M. H. Tawhai, G. McLennan, and E. A. Hoffman. 2009. Computational fluid dynamics. IEEE Eng. Med. Biol. Mag. 28: 25–33.

Loring, S. H., C. R. O'Donnell, N. Behazin, A. Malhotra, T. Sarge, R. Ritz, et al. 2010. Esophageal pressures in acute lung injury: do they represent artifact or useful information about transpulmonary pressure, chest wall mechanics, and lung stress? J. Appl. Physiol. 108:515–522.

Lourens, M. S., B. van den Berg, J. G. Aerts, A. F. Verbraak, H. C. Hoogsteden, and J. M. Bogaard. 2000. Expiratory time constants in mechanically ventilated patients with and without COPD. Intensive Care Med. 26:1612–1618.

Mead, J., T. Takishima, and D. Leith. 1970. Stress distribution pulmonary in lungs: a model of elasticity. J. Appl. Physiol. 28:596–608.

Mentzelopoulos, S. D., C. Roussos, and S. G. Zakynthinos. 2005. Prone position reduces lung stress and strain in severe acute respiratory distress syndrome. Eur. Respir. J. 25:534–544.

Mertens, M., A. Tabuchi, S. Meissner, A. Krueger, K. Schirrmann, U. Kertzscher, et al. 2009. Alveolar dynamics in acute lung injury: heterogeneous distension rather than cyclic opening and collapse. Crit. Care Med. 37:2604–2611.

Nakagawa, S., and H. Schielzeth. 2013. A general and simple method for obtaining R2 from generalized linear mixed-effects models. Methods Ecol. Evol. 4: 133–142.

Otto, C. M., K. Markstaller, O. Kajikawa, J. Karmrodt, R. S. Syring, B. Pfeiffer, et al. 2008. Spatial and temporal heterogeneity of ventilator-associated lung injury after surfactant depletion. J. Appl. Physiol. 104:1485–1494.

da Paula, L. F. S. C., T. Wellman, P. M. Spieth, A. Güldner, J. G. Venegas, M. Gama de Abreu, et al. 2016. Regional tidal lung strain in mechanically ventilated normal lungs. J. Appl. Physioljap. 00861:2015.

Perchiazzi, G., C. Rylander, A. Vena, S. Derosa, D. Polieri, T. Fiore, et al. 2011. Lung regional stress and strain as a function of posture and ventilatory mode. J. Appl. Physiol. 110:1374–1383.

Protti, A., D. Chiumello, M. Cressoni, E. Carlesso, C. Mietto, V. Berto, et al. 2009. Relationship between gas exchange response to prone position and lung recruitability during acute respiratory failure. Intensive Care Med. 35:1011–1017.

Protti, A., M. Cressoni, A. Santini, T. Langer, C. Mietto, D. Febres, et al. 2011. Lung stress and strain during mechanical ventilation: any safe threshold? Am. J. Respir. Crit. Care Med. 183:1354–1362.

Protti, A., D. T. Andreis, M. Monti, A. Santini, C. C. Sparacino, T. Langer, et al. 2013. Lung stress and strain during mechanical ventilation: any difference between statics and dynamics? Crit. Care Med. 41:1046–1055.

Pulletz, S., M. Kott, G. Elke, D. Schädler, B. Vogt, N. Weiler, et al. 2012. Dynamics of regional lung aeration determined by electrical impedance tomography in patients with acute respiratory distress syndrome. Multidiscip. Respir. Med. 7: 1–9.

Santana, M. C. E., C. S. N. B. Garcia, D. G. Xisto, L. K. S. Nagato, R. M. Lassance, L. F. M. Prota, et al. 2009. Prone position prevents regional alveolar hyperinflation and mechanical stress and strain in mild experimental acute lung injury. Respir. Physiol. Neurobiol. 167:181–188.

Schiller, H. J., U. G. McCann, D. E. Carney, L. A. Gatto, J. M. Steinberg, and G. F. Nieman. 2001. Altered alveolar mechanics in the acutely injured lung. Crit. Care Med. 29:1049–1055.

Vos, W., J. De Backer, G. Poli, A. De Volder, L. Ghys, C. Van Holsbeke, et al. 2013. Novel functional imaging of changes in small airways of patients treated with extrafine beclomethasone/formoterol. Respiration 86:393–401.

Vos, W., B. Hajian, J. De Backer, C. Van Holsbeke, S. Vinchurkar, R. Claes, et al. 2016. Functional respiratory imaging to assess the interaction between systemic roflumilast and inhaled ICS/LABA/LAMA. Int. J. Chron. Obstruct. Pulmon. Dis. 11:263–271.

Wolf, G. K., C. Gómez-Laberge, J. S. Rettig, S. O. Vargas, C. D. Smallwood, S. P. Prabhu, et al. 2013. Mechanical ventilation guided by electrical impedance tomography in experimental acute lung injury. Crit. Care Med. 41:1296–1304.